BJP British Journal of Pharmacology

DOI:10.1111/bph.13177
www.brjpharmacol.org

RESEARCH PAPER

Imidazole-based alkaloid derivative LCB54-0009 suppresses ocular angiogenesis and lymphangiogenesis in models of experimental retinopathy and corneal neovascularization

Byung-Hak Kim[1,*], Junyeop Lee[2,†], Jun-Sub Choi[3], Dae Young Park[2], Ho Young Song[4], Tae Kyo Park[4], Chung-Hyun Cho[5], Sang-Kyu Ye[5], Choun-Ki Joo[3], Gou Young Koh[2] and Tae-Yoon Kim[1]

[1]*Department of Dermatology, College of Medicine, The Catholic University of Korea, Seoul, Korea,* [2]*Graduate School of Medical Science and Engineering, Korea Advanced Institute of Science and Technology (KAIST), Daejeon, Korea,* [3]*Catholic Institute for Visual Science and Department of Ophthalmology and Visual Science, College of Medicine, The Catholic University of Korea, Seoul, Korea,* [4]*LegoChem Biosciences, Inc., Daejeon, Korea, and* [5]*Department of Pharmacology and Biomedical Sciences, Seoul National University College of Medicine, Seoul, Korea*

Correspondence
Tae-Yoon Kim, Department of Dermatology, College of Medicine, The Catholic University of Korea, 222 Banpo-daero, Seocho-gu, Seoul 137-701, Korea. E-mail: tykimder@catholic.ac.kr

*Present address: Department of Pharmacology and Biomedical Science Project (BK21[PLUS]), Seoul National University College of Medicine, Seoul, Korea.

†Present address: Department of Ophthalmology, Asan Medical Center, College of Medicine, University of Ulsan, Ulsan, Korea.

Received
20 October 2014
Revised
8 April 2015
Accepted
18 April 2015

BACKGROUND AND PURPOSE

Abnormally induced angiogenesis and lymphangiogenesis are associated with human diseases, including neovascular eye disease. Substances that inhibit these processes may have potential as an attractive therapeutic strategy for these diseases.

EXPERIMENTAL APPROACH

In vitro and *in vivo* angiogenesis and/or lymphangiogenesis were assessed in VEGF- or hypoxia-stimulated endothelial and retinal cells and in animal models of oxygen-induced retinopathy (OIR), streptozotocin-induced diabetic retinopathy (SIDR), suture-induced inflammatory corneal neovascularization (SICNV) and silver nitrate-induced corneal neovascularization. HUVECs and retinal cells were cultured under hypoxic conditions or incubated with VEGF to identify the molecular mechanisms involved.

KEY RESULTS

The imidazole-based alkaloid derivative LCB54-0009 inhibited capillary-like tube formation in VEGF-induced HUVECs without inducing cytotoxic effects. Intravitreal injection of LCB54-0009 into retinas suppressed the formation of the pathological neovascular tufts and increased vascular permeability in both OIR of mice and SIDR of rats. Furthermore, subconjunctival

injection of LCB54-0009 into the cornea suppressed corneal inflammation and inflammation-associated angiogenesis and lymphangiogenesis in SICNV of mice and silver nitrate cauterization of rats. These pharmacological activities were associated with effects on HIF-1α protein stability and HIF-1α/NF-κB redox sensitivity through its antioxidant activities. LCB54-0009 also inhibited the hypoxia-induced expression of angiopoietin-2, and VEGF-induced VEGFR-2 activation and downstream signalling, resulting in the down-regulation of the expression of pro-angiogenic factors and pro-inflammatory mediators and an up-regulation of the expression of anti-angiogenic factors.

CONCLUSIONS AND IMPLICATIONS

LCB54-0009 is a potential candidate molecule for blocking pathological angiogenesis and lymphangiogenesis mediated by HIF-1α- angiopoietin-2 expression and VEGFR-2 activation.

Abbreviations

Ang, angiopoietin; DPPH, 2,2-diphenyl-1-picrylhydrazy; HIF, hypoxia-inducible factor; LCB54-0009, 3-(2-((3,4-dihydroxy-phenyl)-[4-(2-dimethylamino-ethyl)-imidazol-1-yl]-methyl)-benzo[1,3]dioxol-5-yl)-propionic acid; LEC, lymphaticendothelial cell; OIR, oxygen-induced retinopathy; PHD, prolyl hydroxylase; pVHL, von Hippel Lindau protein; ROS, reactive oxygen species; SICNV, suture-induced inflammatory corneal neovascularization; SIDR, streptozotocin-induced diabetic retinopathy; TIMP, tissue inhibitor of metalloproteinase

Tables of Links

TARGETS		
Catalytic receptors[a]	**Enzymes**[b]	
CD11b	COX-2	PHD1 (HIF-2)
TIE-2	iNOS	PHD2 (HIF-1)
TLR2	MMP-1	PHD3
TLR4	MMP-2	Plasminogen (angiostatin)
VEGFR-2	MMP-3	Src
	MMP-9	TSP-1

LIGANDS		
Angiopoietin-2	IL-1β	L-cysteine
Angiostatin	IL-4	LPS
Biotin	IL-6	TIMP1
Histamine	IL-8	TIMP2
Histidine	IL-12	TNF-α
IFN-γ	IL-13	VEGF-A
IL-1α		

These Tables list key protein targets and ligands in this article which are hyperlinked to corresponding entries in http://www.guidetopharmacology.org, the common portal for data from the IUPHAR/BPS Guide to PHARMACOLOGY (Pawson *et al.*, 2014) and are permanently archived in the Concise Guide to PHARMACOLOGY 2013/14 ([a,b]Alexander *et al.*, 2013a,b).

Introduction

Angiogenesis and lymphangiogenesis are complex processes by which endothelial cells (ECs) and lymphatic endothelial cells (LECs) proliferate and migrate from pre-existing blood and lymphatic vessels to form new blood and lymphatic vessels (Adams and Alitalo, 2007; Cao *et al.*, 2013). These newly formed vessels are essential for normal physiological and vital processes, such as growth, development, reproduction, tissue repair, granulation tissue formation, homeostasis, metabolism and immunity. However, pathophysiological angiogenesis and lymphangiogenesis are associated with numerous human diseases, including cancer, vascular disease, inflammatory disease and neovascular eye diseases (Carmeliet and Jain, 2000; Regenfuss *et al.*, 2012). Therefore, drugs that can affect pathological angiogenesis and lymphangiogenesis have potential therapeutic benefits in the prevention of tumour progression and the treatment of vascular, inflammatory and neovascular eye diseases.

Although blood and lymphatic vessels are essential for supplying oxygen and nutrients between tissues and cells, some tissues with a unique structure and function are partly or completely deficient in these vessels under normal conditions. The cornea is one of these rare tissues and an appropriate hypoxic, avascular state is maintained by anti-haemangiogenic factors such as angiostatin, endostatin and thrombospondin 1 (TSP-1; Regenfuss *et al.*, 2012). In contrast, the retina is one of the most metabolically active tissues in the body, and it needs large amounts of oxygen and nutrients to produce metabolic energy. Therefore, ill-timed oxygen levels in the eyes are associated with ocular diseases, such as pathological corneal and retinal haemangiogenesis, lymphangiogenesis, diabetic retinopathy, retinopathy of prematurity (ROP), age-related macular degeneration, high-altitude retinopathy, glaucoma and retinitis pigmentosa, which ultimately lead to vision loss (Arjamaa and Nikinmaa, 2006; Grimm and Willmann, 2012).

Molecular oxygen (O_2) is utilized for the synthesis of ATP. ATP synthesis is essential for metabolic processes, including tissue development, homeostasis and normal physiological function. The cellular O_2 concentration is well-controlled by the vascular system in mammals. However, acute decreases in

these levels cause cellular dysfunction and pathogenesis due to insufficient ATP production, excess reactive oxygen species (ROS) production and hypoxia (Semenza, 2007). Exposure to hypoxia transcriptionally induces a broad range of genes through the induction of oxygen-sensitive hypoxia-inducible factors (HIFs; Kietzmann and Görlach, 2005; Gordan and Simon, 2007; Majmundar *et al.*, 2010). HIF-1α is a master transcription factor in the maintenance of oxygen homeostasis and cellular responses to hypoxia. Short- and long-term exposures to hypoxia induce various genes that are associated with human diseases, including ischaemic cardiovascular disease, hypertension, organ transplant rejection, colitis, ocular neovascularization, hereditary erythrocytosis, inflammatory disease, angiogenesis and cancer (Konisti *et al.*, 2012; Semenza, 2014). In addition, chronic exposure to hypoxia influences drug delivery by altering the expression of drug transporters and the functional activity of carrier transporters (Takagi *et al.*, 1998; Nelson *et al.*, 2003; Wasa *et al.*, 2004; Fradette *et al.*, 2007; Kadam *et al.*, 2013). Therefore, targeting HIFs may be a potential therapeutic strategy for the treatment of many human diseases, including angiogenesis- and lymphangiogenesis-related vascular and neovascular eye diseases.

In addition to histidine, histamine, biotin and alkaloids, the heterocyclic ring of imidazole is an important biological building block. In this study, we identified an imidazole-based alkaloid derivative, 3-(2-((3,4-dihydroxy-phenyl)-[4-(2-dimethylamino-ethyl)-imidazol-1-yl]-methyl)-benzo[1,3] dioxol-5-yl)-propionic acid (LCB54-0009), which exhibited anti-angiogenic and anti-lymphangiogenic activities. This compound effectively inhibited capillary-like tube formation without inducing cytotoxic effects in ECs. In addition, *in vivo* treatment with LCB54-0009 decreased pathological angiogenesis, inflammation and inflammation-associated lymphangiogenesis in animal models of retinopathy and corneal neovascularization. These results were associated with its antioxidant activity, which resulted in the regulation of HIF-1α protein stability and HIF-1α/NF-κB redox sensitivity as well as the inhibition of angiopoietin (Ang) expression and VEGFR-2 signalling cascades. These findings suggest that LCB54-0009 may be a potential molecule for blocking pathological angiogenesis and lymphangiogenesis.

Methods

Cell culture

Primary human umbilical vein endothelial cells (HUVECs) were maintained in EBM-2 medium containing EGM-2 SingleQuots (Clonetics, Walkersville, MD, USA). The spontaneously arising human retinal pigment epithelial cell line ARPE-19 (CRL-2302) was obtained from American Type Culture Collection (ATCC, Manassas, VA, USA) and maintained in DMEM/F-12 medium supplemented with 10% heat-inactivated FBS, 2.5 mM L-glutamine, 15 mM HEPES buffer and antibiotics (100 U·mL^{-1} penicillin and 100 μg·mL^{-1} streptomycin; Invitrogen, Carlsbad, CA, USA). Cells were incubated at 37°C with 5% CO_2 atmosphere in a humidified incubator. Hypoxia was induced in a hypoxic modular incubator chamber with a 94:5:1 mixture of N_2 : CO_2 : O_2, as previously described (Kim *et al.*, 2011).

Preparation of primary retinal cells

Primary retinal pigmented epithelial cells were isolated from the eyes of C57BL/6J mouse as described previously (Grozdanov *et al.*, 2010). Briefly, the retina was isolated from the eye of 6-week-old male C57BL/6J mouse, digested in the digestion solution containing 17 U·mL^{-1} papain (Sigma-Aldrich, St. Louis, MO, USA) and 0.3 g·mL^{-1} L-cysteine (Sigma-Aldrich) in DMEM for 30 min at 37°C, and triturated by sucking it up and down with a Pasteur pipette, followed by removal of the lens, cornea and ciliary body under an inverted microscope. After centrifugation at 600× *g* for 5 min, the cell pellet was suspend in fresh DMEM and cultured at 37°C and 5% CO_2 to maintain the primary retinal cells.

Antioxidant assays

For the antioxidant assays, total antioxidant capacity (TAC), 2,2-diphenyl-1-picrylhydrazyl (DPPH) radical scavenging activity, superoxide radical scavenging activity, nitric oxide (NO) production and peroxynitrite scavenging activity were performed, and the detailed information on experimental procedures is in the Supporting Information.

Tube formation assays

HUVECs were seeded onto the Matrigel (BD Biosciences, San Jose, CA, USA) and incubated with vehicle (0.1% DMSO) or LCB54-0009 (20 μM) in the presence or absence of VEGF (20 ng·mL^{-1}) for 14 h in serum-free conditions. Capillary-like tube formation was assessed using an inverted microscope (Olympus, Japan).

Western blot analysis

Protein samples were separated by SDS-PAGE, and transferred onto PVDF membranes. The membranes were blocked in a blocking buffer containing 5% skimmed milk and incubated with specific primary antibodies for the target molecules overnight at 4°C. Antibodies specific for HIF-1α (ab1), and VEGF (ab46154) were purchased from Abcam (Cambridge, UK). Anti-phospho-VEGFR-2 (#2478), VEGFR-2 (#2479), phospho-p125^{FAK} (#3284), p125^{FAK} (#13009), phospho-Src (#2101), Src (#1587) and GAPDH (#2118) were purchased from Cell Signaling Technology (Danvers, MA, USA), and anti-VHL antibody (SC-17780) was obtained from Santa Cruz Biotechnology (Santa Cruz, CA, USA). The membranes were then incubated with horseradish peroxidase-conjugated secondary antibodies (A24518 and A24537, Life Technologies, Grand Island, NY, USA), and signals were detected using an enhanced chemiluminescence detection kit (iNtRON Biotechnology, Seongnam, Korea).

Quantitative real-time and semi-quantitative reverse transcription PCR

Total RNA was isolated using an RNeasy Mini Kit, and cDNA was synthesized using QuantiTect Reverse Transcription Kit (Qiagen, Valencia, CA, USA). Quantitative real-time PCR (qRT-PCR) was performed using the KAPA SYBR fast qPCR Kit (KAPA Biosystems, Woburn, MA, USA), and the data were normalized to the GAPDH expression. The PCR conditions were one cycle at 95°C for 5 min, followed by 35 cycles of

denaturation at 96°C for 20 s, annealing at 56°C for 20 s, and extension at 72°C for 20 s, and ending with one cycle at 72°C for 5 min. Primers used in this experiment were purchased from Qiagen. Semi-quantitative reverse transcription PCR (RT-PCR) was performed using an RNA PCR kit (Bioneer, Korea), according to the manufacturer's protocols. Total RNA was reverse-transcribed at 42°C for 1 h, and PCR was performed with 25 cycles at 94°C for 30 s, 60°C for 30 s and 72°C for 60 s, and it ended with one cycle at 72°C for 5 min. The products were resolved on agarose gels with DNA SafeStain (Lamda Biotech, St. Louis, MO, USA) by electrophoresis. Primers used in this experiment are summarized in Supporting Information Table S1.

Immunoprecipitation

HUVECs were incubated with deferoxamine (DFX, 200 μM) for 6 h in the presence or absence of LCB54-0009. Whole-cell lysates were pre-cleared with protein A/G-sepharose (Upstate, New York, NY, USA) for 2 h at 4°C and then incubated with 2 μg antibodies in TEG buffer [20 mM Tris–HCl (pH 7.4), 1 mM EDTA, 10% glycerol and 1 mM dithiothreitol] for overnight at 4°C. The immune complexes were precipitated by protein A/G-sepharose beads and washed with TEG buffer containing 0.1% Triton X-100 and then subjected Western blot analysis with appropriate antibodies.

Oxygen-induced retinopathy (OIR) model

All animal care and experimental procedures were conducted in accordance with the National Institute of Health Guide for the Care and Use of Laboratory Animals and were approved by the Animal Care Committee of Korea Advanced Institute of Science and Technology and the Catholic University of Korea. Mice and rats were handled in accordance with the ARVO Statement for the Use of Animals in Ophthalmic and Vision Research. All studies involving animals are reported in accordance with the ARRIVE guidelines for reporting experiments involving animals (Kilkenny *et al.*, 2010; McGrath *et al.*, 2010). All animals were bred and housed in our pathogen-free animal facility, and they were fed with a standard normal diet (PMI Lab diet) *ad libitum* with free access to water. The OIR mouse model was generated, as previously described (Lee *et al.*, 2013). Briefly, newborn C57BL/6J mice ($n = 5$) at P7 and their nursing mothers were exposed to 75% oxygen in a hyperoxic chamber (ProOx Model 110, Biospherix, Lacona, NY, USA) for 5 days, after which they were returned to room air for 5 days.

Suture-induced inflammatory corneal neovascularization (SICNV) model

The SICNV model was generated according to a previous report (Bock *et al.*, 2007) with some modifications. Briefly, 8-week-old male C57BL/6J mice ($n = 5$) were anaesthetized with an i.m. injection of ketamine (40 mg·kg^{-1}) and xylazine (12 mg·kg^{-1}). One 10-0 nylon suture (Ethicon, Somerville, NJ, USA) was placed intrastromally. The outer point of suture placement was placed near the limbus, and the inner suture point was positioned near the corneal centre that was equidistant from the limbus. Vehicle (0.1% DMSO per 10 μL), LCB54-0009 (100 μg per 10 μL) or VEGF trap (100 μg per 10 μL) was subconjunctivally injected on the day of suture placement. After 2 weeks, the mice were killed.

Silver nitrate-induced corneal neovascularization model

Sprague-Dawley male rats weighing 250 g ($n = 5$) were anaesthetized by an i.p. injection of ketamine hydrochloride (20 mg·kg^{-1}) and xylazine hydrochloride (2.5 mg·kg^{-1}). The centres of the right corneas were then cauterized with a silver nitrate applicator stick (75% silver nitrate and 25% potassium nitrate), which was held in contact with the cornea (1 mm diameter) for 10 s. Three days after cauterization, vehicle (1% DMSO per 20 μL), LCB54-0009 (50 μg per 20 μL) or Avastin (200 μg per 20 μL) was injected into the subconjunctiva. The inhibitory effect was observed under an ophthalmic microscope (Carl Zeiss, Jena, Germany) with a digital camera. The images captured were analysed using ImageJ software.

Histological analysis

Immunohistochemistry in whole-mounted retinas or corneas was performed as previously described (Bock *et al.*, 2007). The retina was incubated with hamster anti-CD31 monoclonal antibody (Millipore, Billerica, MA, USA) or with one or more of the following antibodies: rat anti-TER119 monoclonal antibody (clone TER-119, BD Biosciences), rabbit anti-lymphatic vessel endothelial receptor (LYVE)-1 polyclonal antibody (AngioBio, Del Mar, CA, USA) or rat anti-CD11b monoclonal antibody (clone M1/70, BD Biosciences). After several washes, the samples were incubated for 4 h at room temperature with cyanine 3 (Cy3)-conjugated anti-hamster immunoglobulin G (IgG), Cy5-conjugated anti-rat IgG, or FITC-conjugated anti-rabbit IgG (Jackson ImmunoResearch, West Grove, PA, USA). Flat-mount stained retinas or corneas were visualized, and digital images were obtained using a Zeiss LSM 510 confocal microscope equipped with argon and helium-neon lasers (Carl Zeiss).

Morphometric analysis

Morphometric analysis on the retina and cornea was performed using the ImageJ software or LSM Image Browser (Carl Zeiss). Neovascular tufts (NVTs) and avascular areas in OIR retinas were measured using the Lasso tool of the Adobe Photoshop software, as previously described (Connor *et al.*, 2009). The numbers of extravasated Ter119^{+} erythrocytes were counted in four random 0.2 mm^2 areas of each retina. Retinal vascular permeability was determined using FITC-labelled dextran. The area extravasated dextran was calculated as the FITC-dextran-positive area divided by the total retinal area in each quadrant of retinal mount, and it is presented as a percentage. Vessel diameters on the cornea were averaged from all CD31 positive blood vessels that were located at the halfway point between the outer point of suture placement and the limbus. The blood or lymphatic vascular density in whole-mounted corneas was calculated as the area of CD31 positive blood vessels or LYVE-1 positive lymphatic vessels divided by the total corneal area measured per 0.2 mm^2 field, and it is presented as a percentage. The macrophage infiltration area was calculated by measuring the CD11b positive area per 0.02 mm^2 field of each site of suture placement.

Statistics

Values are presented as mean ± SD of three independent experiments ($n = 3$). Statistical differences were determined by one-way ANOVA followed by Dunnett's multiple comparison tests. Differences were considered to be statistically significant at $P < 0.05$.

Results

Synthesis of imidazole-based alkaloids

Only a small population of alkaloids contains the imidazole nucleus. However, these imidazole-based alkaloids have been shown to exhibit multiple biological activities, such as anti-tuberculosis, antibacterial, anti-fungal and anti-inflammation (Rivers and Mancera, 2008; Duan *et al.*, 2013; Kong *et al.*, 2013; Castelli *et al.*, 2014). To develop novel compounds possessing pharmacological properties that exhibit anti-angiogenic and anti-lymphangiogenic activities, we synthesized imidazole-based alkaloid derivatives from 3,4-dihydroxybenzaldehyde (Supporting Information Fig. S1, ≥97% purity). The synthetic procedures, ^{1}H- and ^{13}C-NMR and LC-MS spectra of intermediates and LCB54-0009 are shown in Supporting Information Fig. S2–S4 and have been previously described (Song *et al.*, 2012). The functional groups of L and M are –H, –OH or –OR, and R is C_{1-4} alkyl. The X and Y are carbon or nitrogen, and m is 0~4. The R^1 is –H, –OH, $-OR^3$, $-NR^3R^4$, $-NR^3(C(O)R^4)$, $-NR^3(SO_2R^4)$, $-NR^3(CO_2R^4)$, $-NR^3(C(O)NR^3R^4)$, –CN, $-CO_2R^3$ or $-C(O)NR^3R^4$, and R^3 and R^4 are –H or C_{1-6} alkyl. The R^2 is –H, –F, –Cl, –Br, –OH, $-OR^5$, $-OSO_3R^5$, $-CF^3$, $-OCF^3$, –C(O)Me, –CN, $-CO_2R^5$, $-C(O)NR^5R^6$, $-SO_3R^5$, $-SO_2NR^5R^6$, $-(CH{=}CH)CO_2R^5$, $-(CH{=}CH)C(O)NR^5R^6$, $-(CH{=}CH)SO_3R^5$, $-(CH{=}CH)CH_2OH$, $-R^5$, $-R^5OR^6$, $-R^5OSO_3R^6$, $-R^5CO_2R^6$, $-R^5C(O)NR^6R^7$, $-R^5SO_3R^6$ or $-R^5SO_2NR^6R^7$, and R^5, R^6 and R^6 are –H, C_{1-6} alkyl, or C_{2-6} alkylene. All of the compounds contain two chiral carbons and LCB54-0002 and LCB54-0003, LCB54-0008 and LCB54-0009, and LCB54-0016 and LCB54-0017 are identified as isomers. We performed *in vitro* and *in vivo* experiments to identify potential candidate molecules. The data show that LCB54-0007, LCB54-0009 and LCB54-0012 exhibited effective anti-angiogenic activity in models of streptozotocin-induced diabetic retinopathy (SIDR) and silver nitrate-cauterized corneal neovascularization (Supporting Information Fig. S5). In addition, these three molecules exhibited more potential antioxidant activity than other molecules, while all of the compounds exhibited marginal to weak peroxynitrite scavenging activity (Supporting Information Fig. S6). We also determined their effects on hypoxia-induced increased levels of HIFs and LCB54-0009 exhibited the strongest inhibition of the increase in HIF-1α without affecting HIF-2α levels (Supporting Information Fig. S7b). We therefore selected LCB54-0009 (Figure 1A) as a potential target molecule for further studies and to elucidate the mechanisms involved in its anti-angiogenic activity. Structure–activity relationship analysis suggested that the number of hydroxyl groups in the catechol plays an important role in its antioxidant activity and the methyl group in the amine as well as the carboxylic group in the benzo[1,3]dioxole may be important factors for determining their biological activities.

LCB54-0009 exhibits anti-angiogenic activity in vitro

We first performed a tube formation assay to identify the *in vitro* anti-angiogenic activity of LCB54-0009 because this phenomenon is a well-known, essential step for angiogenesis. Capillary-like tube formation was increased in VEGF-stimulated HUVECs, compared with the vehicle-treated group. LCB54-0009 effectively inhibited this angiogenic activity (Figure 1B). In parallel with this effect, LCB54-0009 reduced the mRNA levels of pro-angiogenic factors, including VEGF-A, MMPs (MMP-1, MMP-2, MMP-3 and MMP-9) and cluster of differentiation 31 (CD31). In contrast, LCB54-0009 increased the mRNA levels of the tissue inhibitors of metalloproteinases, TIMP-1 and TIMP-2, which are anti-angiogenic factors (Figure 1C). Interestingly, treatment with 100 μM LCB54-0009 over a 72-h period did not affect the viability of HUVECs, ARPE-19 and primary retinal cells isolated from the eyes of C57BL/6J mouse (Figure 1D and Supporting Information Fig. S7A).

LCB54-0009 suppresses pathological angiogenesis and vascular leakage in vivo

To investigate the *in vivo* anti-angiogenic activity of LCB54-0009 in the retina, we generated the OIR mouse model, which mimics human retinopathy of prematurity (ROP) and certain aspects of proliferative diabetic retinopathy (Frank, 2004; Sapieha *et al.*, 2010). The retinas of OIR mice developed extensive vascular regression in the central region and pathological NVTs in the middle and peripheral regions. Intravitreal injection of LCB54-0009 (10 μg) or VEGF trap (10 μg) effectively suppressed NVT formation, compared with that of fragment crystallizable (Fc)-injected group (Figure 2A–C).

To measure vascular leakage, we injected FITC-dextran i.v. into OIR mice, 1 h before they were killed. Some extravasated FITC-dextran was detected within the retina near the NVTs in control mice. The regions where FITC-dextran was most abundant matched the locations of extravasated Ter119^{+} erythrocytes, indicating ongoing leakage at the sites of haemorrhage. The degree of FITC-dextran leakage was markedly decreased by the intravitreal injection of LCB54-0009 or VEGF trap (Figure 2D–F), which suggests that LCB54-0009 suppresses pathological angiogenesis and vascular leakage in the OIR mouse model. These results indicate that LCB54-0009 significantly decreases retinal vascular permeability in pathogenic angiogenesis.

LCB54-0009 suppresses corneal neovascularization and inflammation-associated lymphangiogenesis in vivo

The aforementioned results encouraged us to determine whether LCB54-0009 may also affect corneal inflammation and neovascularization. We generated a SICNV mouse model, which develops extensive blood and lymphatic vessel proliferations that originate from the limbus to the suture site (Bock *et al.*, 2007). Haemangiogenesis and lymphangiogenesis were induced by suture-induced corneal inflammation. Subconjunctival injection of LCB54-0009 (100 μg) or VEGF-trap (100 μg) effectively suppressed haemangiogenesis, lym-

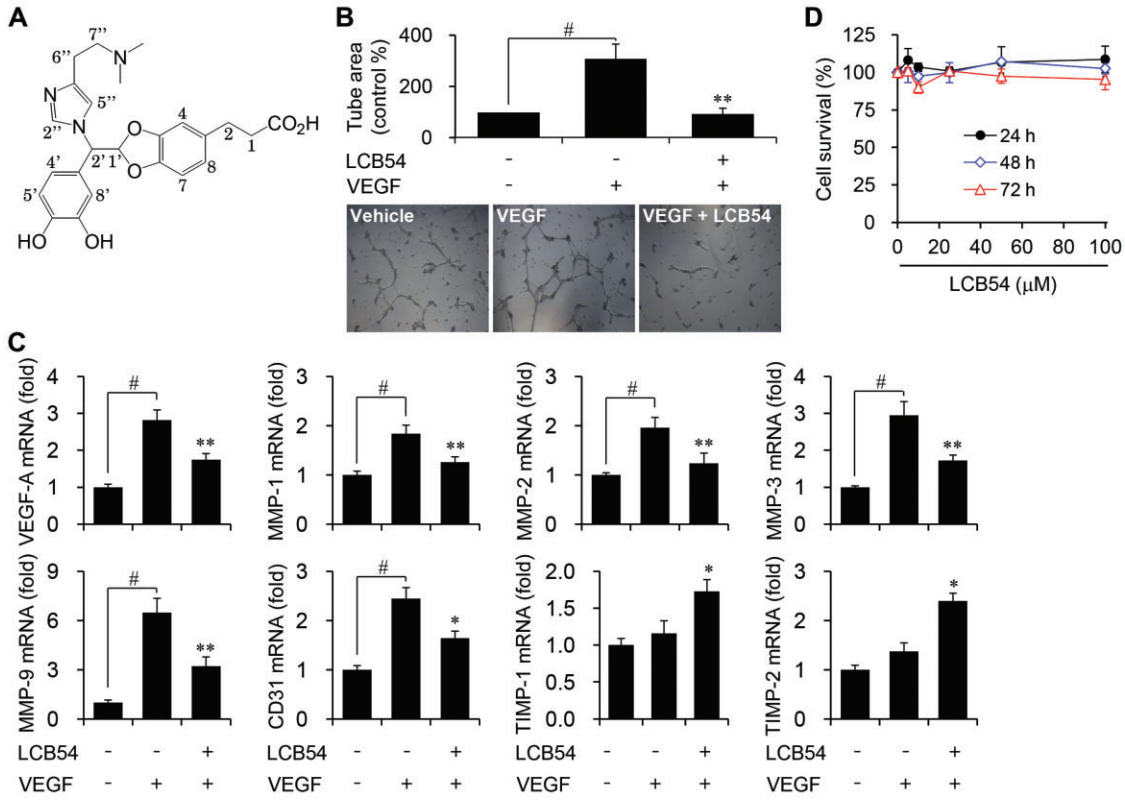

Figure 1

LCB54-0009 inhibits VEGF-induced angiogenesis *in vitro*. (A) Chemical structure of LCB54-0009 ($C_{24}H_{27}N_3O_6$, MW = 453.49, ≥97% purity). (B) Serum-starved HUVECs were seeded onto the Matrigel and incubated with vehicle (0.1% DMSO) or LCB54-0009 (20 μM) in the presence or absence of VEGF (20 ng·mL^{-1}) for 14 h. Capillary-like tube formation was viewed by using an inverted microscope. (C) HUVECs were incubated with vehicle (0.1% DMSO) or LCB54-0009 (20 μM) in the presence or absence of VEGF (20 ng·mL^{-1}) for 48 h. The mRNA levels were determined by quantitative real-time PCR. (D) HUVECs were incubated with various concentrations of LCB54-0009 for 24 to 72 h and cell viability was measured using the WST-1 reagent. Results are expressed as the mean ± SD of three independent experiments (n = 3). #P < 0.05 versus vehicle-treated group; *P < 0.05 and **P < 0.005 versus VEGF-stimulated group.

phangiogenesis and the infiltration of CD11b positive inflammatory cells, compared with the Fc-treated group (Figure 3A–E). This indicates that LCB54-0009 suppresses corneal inflammation and inflammation-associated angiogenesis and lymphangiogenesis.

The effects of LCB54-0009 were also examined in a rat corneal angiogenesis model, in which the centres of the right corneas were cauterized with a silver nitrate applicator stick. After 2 weeks of cauterization, new vessels covered the full cornea. However, new vessels were observed in the quarter-cornea region in the LCB54-0009 (50 μg)- and Avastin (200 μg)-treated corneas. The mean percentages of the neovascularized area were greatly reduced in the LCB54-0009 treated groups compared to the control (Figure 3F and G). These findings indicate that LCB54-0009 has an inhibitory effect on corneal neovascularization and inflammation.

LCB54-0009 inhibits HIF-1α levels

Low oxygen levels induce a wide range of genes through the up-regulation of HIFs that are associated with angiogenesis, lymphangiogenesis, metastasis and inflammation (Cao, 2005; Tammela and Alitalo, 2010). Our preliminary results revealed that among the derivatives, LCB54-0009 exhibited the strongest inhibition of HIF-1α expression without affecting HIF-2α levels (Supporting Information Fig. S7B). To elucidate the molecular mechanisms of the anti-angiogenic and anti-lymphangiogenic activities of LCB54-0009, we first determined whether LCB54-0009 could inhibit the expression of oxygen-sensitive master transcription factors HIFs. The levels of HIF-1α were markedly elevated in HUVECs, ARPE-19 and primary retinal cells under hypoxic conditions. LCB54-0009 inhibited these elevated levels of HIF-1α in a concentration-dependent manner, ultimately resulting in the down-regulation of VEGF levels. However, HIF-1α levels were restored in the presence of the protease inhibitor, carbobenzoxy-Leu-Leu-leucinal (MG-132) (Figure 4A–C and Supporting Information Fig. S7C). HIFs can activate the transcription of numerous pro-angiogenic factors and pro-inflammatory mediators (Kelly *et al.*, 2003; Simon *et al.*, 2008; Semenza, 2013). We therefore performed quantitative real-time PCR to identify the effects of LCB54-0009 on the

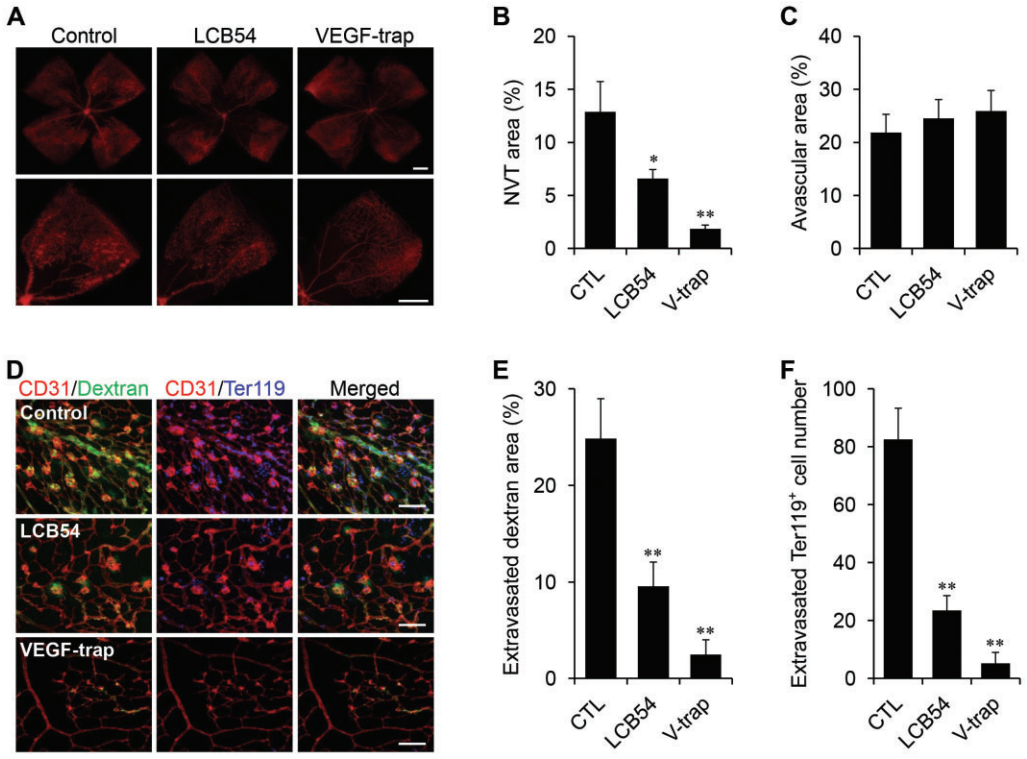

Figure 2

LCB54-0009 suppresses pathological angiogenesis and vascular leakage. (A–C) Intravitreal injection of vehicle (0.1% DMSO), LCB54-0009 (10 μg) or VEGF-trap (10 μg) in OIR mice (n = 5 per group). Vascular regression in the central region (A), pathological NVTs (B) and avascular area (C) were measured in the middle and peripheral regions of the retinas. Scale bars = 200 μm. (D–F) FITC-dextran was injected i.v. 1 h before the OIR mice were killed (D). Extravasated FITC-dextran (E) and extravasated Ter119$^+$ cells (F) were measured within the retina near the NVT. Scale bars = 100 μm. *P < 0.05 and **P < 0.005 versus control mice. CTL, control; LCB54, LCB54-0009; V-trap, VEGF trap.

expression of angiogenic factors and inflammatory mediators. LCB54-0009 significantly inhibited the mRNA levels of pro-angiogenic factors, including VEGF-A and MMPs (Figure 4D and Supporting Information Fig. S8) and pro-inflammatory molecules, including IL-1α, IL-4, IL-6, IL-8, IL-12, IL-13, COX-2 and inducible NOS (iNOS), compared with those of hypoxia-stimulated HUVECs, ARPE-19 and primary retinal cells. The expression levels of these factors and mediators were restored in the presence of MG-132 (Figure 4E).

LCB54-0009 regulates HIF-1α stability and HIF-1α/NF-κB redox sensitivity

HIF-1α stability is regulated by oxygen levels, which affect the activity of prolyl hydroxylases (PHDs) and von Hippel Lindau protein (pVHL; Lee *et al.*, 2004; Ke and Costa, 2006). In addition, many stimuli, including growth factors, LPS, cytokines, thrombin and insulin can induce HIF-1α expression under normoxic conditions through ROS production and redox-sensitive transcription factor NF-κB (Zelzer *et al.*, 1998; Richard *et al.*, 2000; Görlach *et al.*, 2001; Haddad and Land, 2001; Blouin *et al.*, 2004; Bonello *et al.*, 2007; Görlach and Bonello, 2008). We examined whether the inhibitory effect of LCB54-0009 on HIF-1α protein levels is associated with transcription levels and/or HIF-1α/NF-κB redox sensitivity. Interestingly, although the mRNA levels of HIF-1α were not affected by LCB54-0009, this compound inhibited the mRNA levels of PHD3, but not PHD1 and PHD2 (Figure 5A and Supporting Information Fig. S9A), suggesting that it may regulate HIF-1α stability by pVHL. pVHL is a tumour suppressor protein that targets HIF-1α for oxygen-dependent proteolysis (Maxwell *et al.*, 1999). LCB54-0009 increased the interaction between HIF-1α and pVHL, compared with DFX (hypoxia-mimetic agent)-treated cells (Figure 5B). In addition, the ubiquitinated levels of HIF-1α protein were increased in LCB54-0009-treated cells (Figure 5C). We also observed that LCB54-0009 inhibited the mRNA levels of Toll-like receptors (TLR2 and TLR4) and NF-κB subunits p50 and p65, while these levels were restored in the presence of MG-132 (Figure 5D), indicating that LCB54-0009 affects HIF-1α protein stability and HIF-1α/NF-κB redox sensitivity.

LCB54-0009 exhibits antioxidant activity

Hypoxia increases ROS levels, which perturb the balance between cellular antioxidants and pro-oxidants. Antioxidants exhibit anti-angiogenic activity by affecting HIF-1α stability

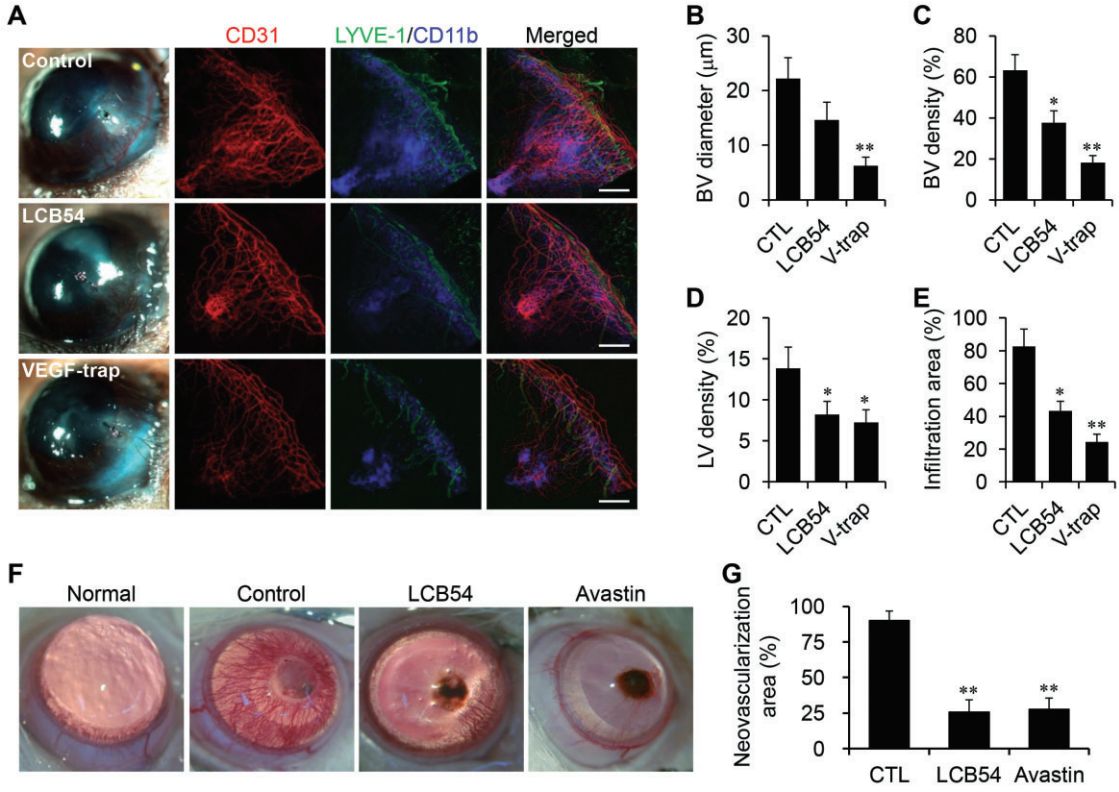

Figure 3

LCB54-0009 inhibits corneal neovascularization and inflammation-associated lymphangiogenesis. (A–E) Proliferation of blood vessels (BV) and lymphatic vessels (LV) were generated in the SICNV mouse model ($n = 5$ per group). Vehicle (0.1% DMSO), LCB54-0009 (100 μg) or VEGF trap (100 μg) was injected subconjunctivally on the day of corneal suture placement. Corneal angiogenesis, lymphangiogenesis and inflammation were determined by staining with CD31 (red), LYVE-1 (green) and CD11b (blue) antibodies respectively (A). BV diameter (B), BV density (C), LV density (D) and the infiltration area of inflammatory cells (E) were measured. Scale bars = 500 μm. (F and G) Corneal neovascularization was induced by the subconjunctival injection of silver nitrate to cauterize the cornea of rats ($n = 5$ per group). Vehicle (1% DMSO), LCB54-0009 (50 μg) or Avastin (200 μg) was injected subconjunctivally three days after silver nitrate cauterization and measured using an ophthalmic microscope with a digital camera. Original magnification was ×100. Avastin was used as a positive control. *$P < 0.05$ and **$P < 0.005$ versus control mice. CTL, control; LCB54, LCB54-0009; V-trap, VEGF trap.

and HIF-1α/NF-κB redox sensitivity (Haddad *et al.*, 2000; Gao *et al.*, 2007; Park *et al.*, 2010; Sceneay *et al.*, 2013). To investigate the possible antioxidant effects of LCB54-0009, we first measured the total antioxidant capacity (TAC). LCB54-0009 exhibited effective TAC activity with an IC_{50} value of 15.8 μM (Figure 6A). In addition, the imidazole-based alkaloid derivatives all exhibited DPPH radical scavenging activity, except for LCB54-0016 and LCB54-0017. Among them, LCB54-0009 exhibited the strongest DPPH radical scavenging activity with an IC_{50} value of 8.3 μM (Supporting Information Fig. S6 and Figure 6B). To determine the ROS scavenging activities, we performed a non-enzymatic assay of superoxide radicals and assessed their radical scavenging activities. LCB54-0009 scavenged superoxide radicals with an IC_{50} value of 15.5 μM (Figure 6C). To further investigate whether LCB54-0009 could affect the production of reactive nitrogen species (RNS), we performed the Griess reaction to measure NO production. The levels of nitrites, the stable NO metabolites, were increased by more than fivefold by stimulation of HUVECs for 36 h with LPS, TNF-α, IL-1β and IFN-γ; LCB54-0009 exhibited an inhibitory effect against NO production with an IC_{50} value of 10.5 μM; this effect was mediated via inhibition of the levels of iNOS, an inducible enzyme producing large amounts of NO (Figure 6D and Supporting Information Fig. S9B). However, our synthetic derivatives, including LCB54-0009 (up to 50 μM) did exhibit weak peroxynitrite scavenging activity (Supporting Information Figs S6A and S9C). These results clearly indicate that the antioxidant activities of LCB54-0009 result in its inhibitory effects on HIF-1α stability and HIF-1α/NF-κB redox sensitivity.

LCB54-0009 inhibits Ang-2 levels and VEGFR-2-signalling cascades

The Ang/Tie pathway also regulates angiogenesis, and Ang-2 is increased by exposure to hypoxia (Yuan *et al.*, 2000; Felcht *et al.*, 2012; Fagiani and Christofori, 2013). Although, Ang-2 is known to inhibit angiogenesis by binding with TIE-2, which interacts with integrins to induce angiogenesis (Felcht

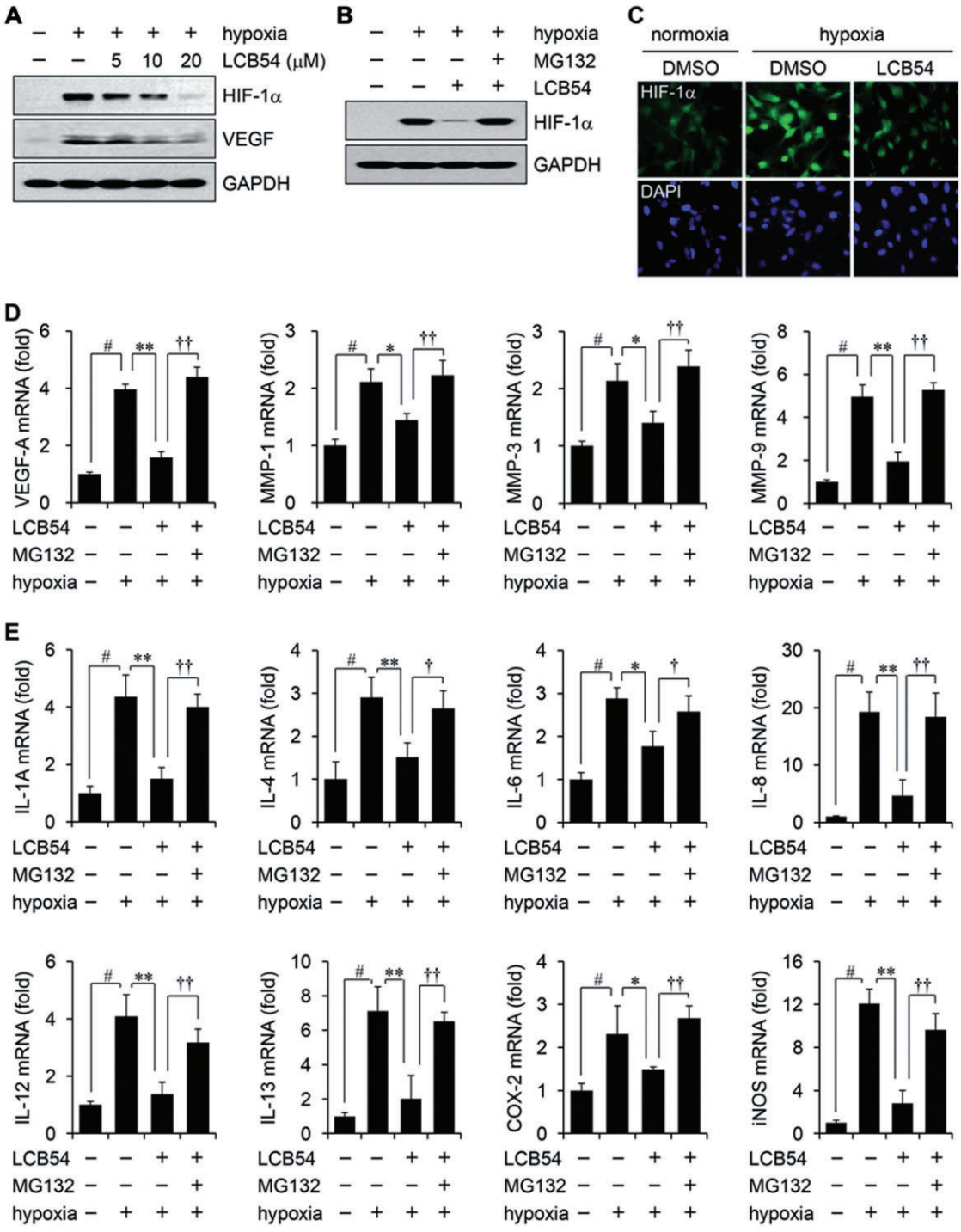

Figure 4

LCB54-0009 inhibits hypoxia-induced increased levels of HIF-1α, angiogenic factors and inflammatory mediators. HUVECs were incubated with LCB54-0009 for 6 h in hypoxia. (A–C) HIF-1α levels were determined by Western blotting (A and B) or immunofluorescence (C). GAPDH served as a loading control. (D and E) The mRNA levels of angiogenic factors (D) and inflammatory mediators (E) were determined by quantitative real-time PCR. Results are expressed as the mean ± SD of three independent experiments ($n = 3$). #$P < 0.05$ versus vehicle-treated group; *$P < 0.05$ and **$P < 0.005$ versus hypoxia-induced group; $^{\dagger}P < 0.05$ and $^{\dagger\dagger}P < 0.005$ versus LCB54-0009-treated group.

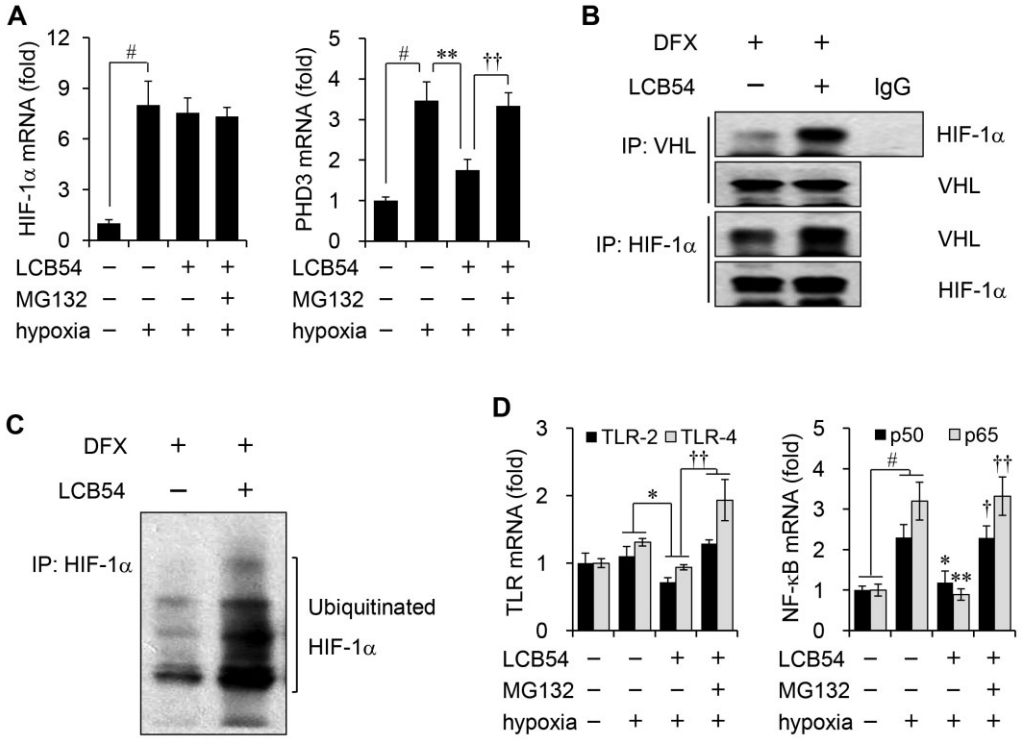

Figure 5

LCB54-0009 regulates HIF-1α stability and HIF-1α/NF-κB redox sensitivity. (A and D) HUVECs were incubated for 6 h in hypoxia and the mRNA levels were determined by quantitative real-time PCR. Results are expressed as the mean ± SD of three independent experiments ($n = 3$). #$P < 0.05$ versus vehicle-treated group; *$P < 0.05$ and **$P < 0.005$ versus hypoxia-induced group; †$P < 0.05$ and ††$P < 0.005$ versus LCB54-0009-treated group. (B and C) HUVECs were incubated with DFX (200 μM) in the presence or absence of LCB54-0009 (20 μM) in hypoxia for 6 h. Anti-VHL or anti-HIF-1α immunoprecipitates were analysed by Western blot analysis.

et al., 2012). Targeting Ang/Tie with VEGF signalling pathways has recently emerged to have valuable therapeutic potential for anti-angiogenic therapy. Ang-2 expression was increased in either hypoxia- or VEGF-treated HUVECs, whereas Ang-1 expression was increased by VEGF stimulation. Treatment with LCB54-0009 effectively decreased the levels of Ang-2, which resulted in the inhibition of VEGF-A levels (Figure 7A–C). The inhibition of hypoxia-induced Ang-2 levels by LCB54-0009 suggests that this molecule may affect the binding of integrins with TIE-2 rather than that of Ang-2 and TIE-2. Interestingly, LCB54-0009 inhibited the tyrosine phosphorylation of VEGFR-2 without altering its mRNA and protein levels in either hypoxia- or VEGF-stimulated HUVECs, thus resulting in the inhibition of its downstream signalling targets, such as $p125^{FAK}$ and Src in VEGF-stimulated HUVECs (Figure 7C and D). However, this compound did not inhibit VEGFR-2 kinase activity (data not shown). The results indicate that the inhibitory effect of LCB54-0009 on Ang-2 expression and VEGFR-2 activation may also contribute to its anti-angiogenic activity.

Discussion and conclusions

Large numbers of imidazole derivatives have been synthesized in the field of medicinal chemistry and are being developed for different pharmacological effects, including antifungal, antibacterial, analgesic, anti-inflammatory, anticancer, cardiovascular, anti-neoplastic, anti-tuberculosis and enzyme-inhibitory activities (Rivers and Mancera, 2008; Duan *et al.*, 2013; Kong *et al.*, 2013; Castelli *et al.*, 2014). In this study, we identified an imidazole-based alkaloid derivative LCB54-0009 as a potential inhibitor molecule for pathological angiogenesis and inflammation-associated lymphangiogenesis.

HIFs are oxygen sensors that are induced under low oxygen levels. They induce the transcription of numerous signalling factors, including pro-angiogenic and pro-inflammatory molecules (Kelly *et al.*, 2003; Simon *et al.*, 2008; Semenza, 2013); these molecules, by interacting with their cognate receptors on blood vessel endothelial cells, LECs, bone marrow-derived cells and inflammatory cells, lead to inflammation, inflammation-associated angiogenesis and lymphangiogenesis, and tumour metastasis (Cao, 2005; Tammela and Alitalo, 2010). In addition, lymphangiogenesis exacerbates inflammatory diseases and graft rejections (Cueni and Detmar, 2006; Norrmén *et al.*, 2011; Semenza, 2013). Therefore, HIFs are important therapeutic targets for the prevention and treatment of pathogenic angiogenesis and lymphangiogenesis. We synthesized a series of imidazole-based alkaloid derivatives to identify small molecule inhibitors that target HIF-mediated signalling cascades to exert anti-

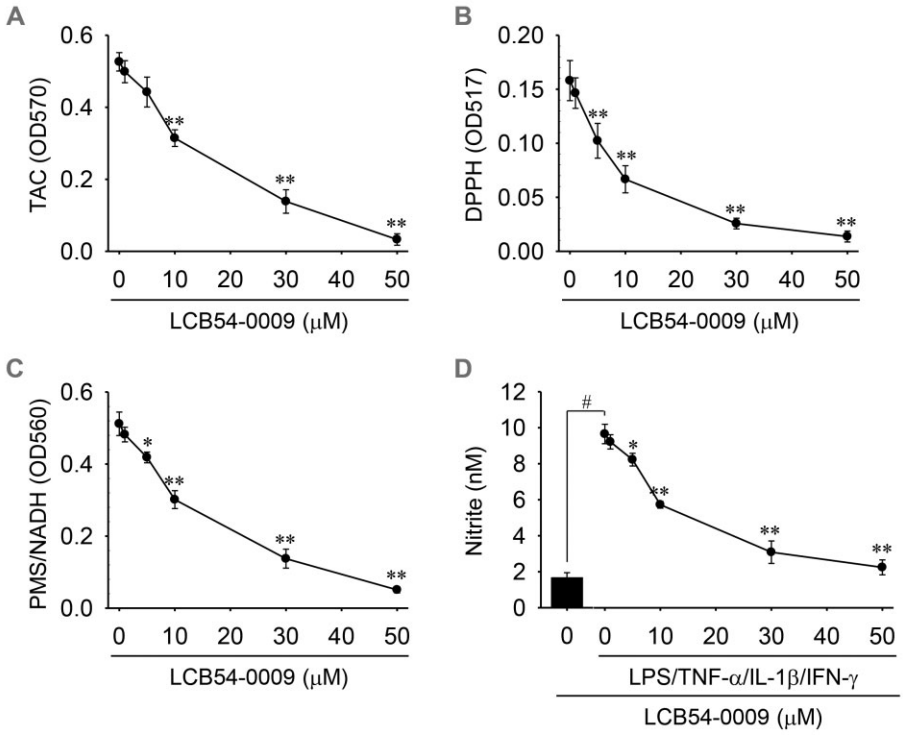

Figure 6

LCB54-0009 exhibits antioxidant activities. (A) The mixtures of hypoxia-stimulated HUVEC lysates, LCB54-0009 and Cu^{2+}-containing working solution were incubated at room temperature for 1.5 h. Total antioxidant capacity (TAC) was measured as absorbance at 570 nm. (B) LCB54-0009 was mixed with DPPH solution and the mixtures were incubated at 25°C for 30 min. DPPH radical scavenging activity was measured as absorbance at 517 nm. (C) Superoxide radical was produced by the NADH/PMS system and the scavenging activity was measured as absorbance at 567 nm, followed by incubation at 25°C for 5 min. (D) HUVECs were incubated with LCB54-0009 in combination with stimuli (LPS 1 $\mu g \cdot mL^{-1}$, TNF-α 10 $ng \cdot mL^{-1}$, IL-1β 5 $U \cdot mL^{-1}$ and IFN-γ 100 $U \cdot mL^{-1}$) for 36 h. Amounts of NO were measured using a Griess reaction. Results are expressed as the mean ± SD of three independent experiments ($n = 3$). *$P < 0.05$ and **$P < 0.005$ versus control group (A–C); #$P < 0.05$ versus vehicle-treated group; *$P < 0.05$ and **$P < 0.005$ versus stimuli-induced group (D).

angiogenic and anti-lymphangiogenic activities. Among the derivatives, LCB54-0009 significantly inhibited the levels of HIF-1α protein in hypoxia-induced HUVECs. This resulted in the down-regulation of VEGF levels and capillary-like tube formation in either hypoxia- or VEGF-stimulated HUVECs, mediated through the suppression of the mRNA levels of various pro-angiogenic and pro-inflammatory molecules and the up-regulation of the mRNA levels of anti-angiogenic molecules. We further observed that LCB54-0009 suppressed pathological angiogenesis and inflammation-associated lymphangiogenesis in animal models of hypoxia-induced retinopathy, diabetic retinopathy and corneal neovascularization.

The stability of HIF-1α protein is regulated by oxygen balance. HIF-1α protein undergoes rapid degradation under normoxic conditions by being processed by the PHD/pVHL-mediated ubiquitin-proteasome pathway, whereas it is protected from degradation under hypoxic conditions (Lee *et al.*, 2004; Ke and Costa, 2006). Numerous growth factors and cytokines as well as NO have been reported to stabilize HIF-1α under normoxic conditions (Zelzer *et al.*, 1998; Richard *et al.*, 2000; Görlach *et al.*, 2001; Haddad and Land, 2001; Blouin *et al.*, 2004; Lee *et al.*, 2004; Ke and Costa, 2006; Bonello *et al.*, 2007; Görlach and Bonello, 2008). In addition, ROS released from a functional electron transport chain stabilize HIF-1α protein (Haddad and Land, 2001; Hagen, 2012), indicating the importance of controlling intracellular oxygen, ROS and RNS levels for HIF-1α stabilization. The factors that regulate HIF-1α stabilization are associated with activation of the transcription factor NF-κB, which binds to a distinct element in the proximal promoter of the HIF-1α gene (Bonello *et al.*, 2007; Görlach and Bonello, 2008). These findings imply that one possible mechanism underlying HIF-1α expression and stabilization is regulated by antioxidants and at the transcription level by the redox-sensitive transcription factor NF-κB. Interestingly, our results revealed that LCB54-0009 is able to mediate antioxidant activities, which may contribute to the regulation of HIF-1α stability and HIF-1α/NF-κB redox sensitivity.

The formation of blood and lymphatic vessels under well-controlled angiogenic and lymphangiogenic processes is important in normal physiological conditions and performs a vital functions. However, when abnormal or dysfunctional, these processes are associated with numerous human diseases (Carmeliet and Jain, 2000; Regenfuss *et al.*, 2012). LCB54-

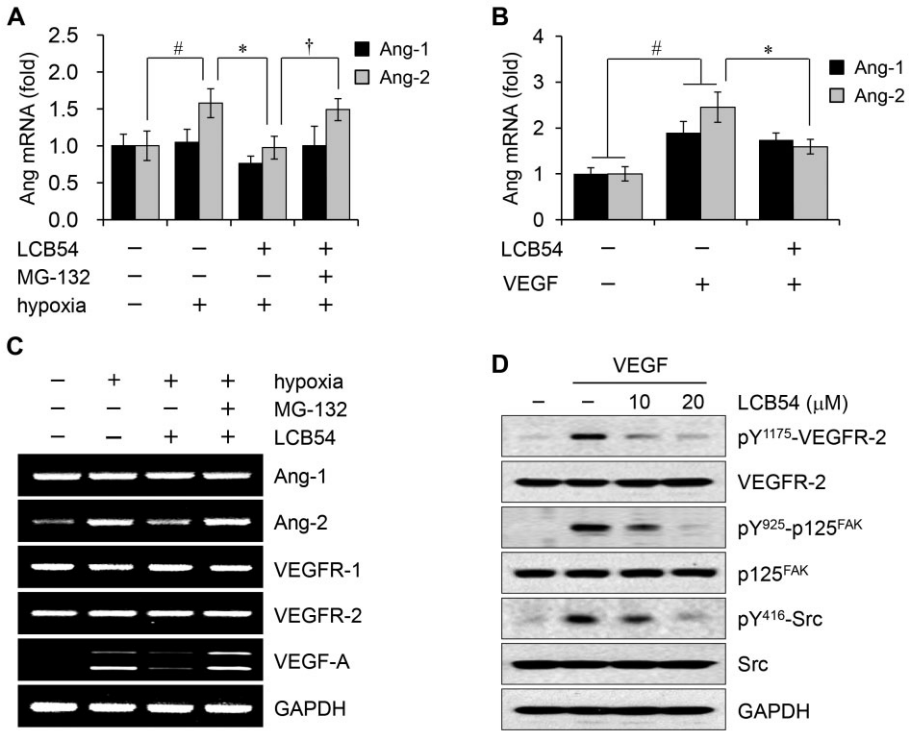

Figure 7

LCB54-0009 inhibits Ang-2 levels and VEGFR-2-signalling cascades. (A–C) HUVECs were incubated for 6 h in hypoxia or 48 h with VEGF (20 ng·mL^{-1}) in the presence or absence of LCB54-0009 (20 μM). The mRNA levels were determined by quantitative real-time PCR (A and B) or reverse transcription PCR (C). Results are expressed as the mean ± SD of three independent experiments ($n = 3$). #$P < 0.05$ versus vehicle-treated group; *$P < 0.05$ versus hypoxia- or VEGF-induced group; †$P < 0.05$ versus LCB54-0009-treated group. (D) HUVECs were incubated with LCB54-0009 for 1 h and then stimulated with VEGF (20 ng·mL^{-1}) for 15 min. Western blotting was performed from the cell lysates. GAPDH served as a loading control.

0009 also suppressed angiogenesis and inflammation-associated lymphangiogenesis, as demonstrated by its inhibition of capillary-like tube formation in VEGF-stimulated HUVECs and retinopathy and corneal neovascularization in animal models of inflammation. VEGF is a well-known, pro-angiogenic factor that binds to its receptor to increase vascular permeability and promote vasculogenesis and angiogenesis by stimulating EC sprouting and proliferation. There are five members of VEGFRs: VEGFR-1, VEGFR-2, VEGFR-3, neuropilin-1 and neuropilin-2. Of these, VEGFR-2 is the most important receptor for VEGF-A-induced angiogenesis in vascular ECs (Ferrara *et al.*, 2003; Roskoski, 2007). The phosphorylation of VEGFR-2 at specific tyrosine residues by VEGF-A activates its down-signalling cascades (Olsson *et al.*, 2006; Holmes *et al.*, 2007). LCB54-0009 effectively inhibited the phosphorylation of VEGFR-2, but not its kinase activity, in VEGF-stimulated ECs, which resulted in the inhibition of its down-signalling cascades. Furthermore, we found that LCB54-0009 inhibited Ang-2 expression in either hypoxia- or VEGF-stimulated ECs, suggesting that the Ang-2-mediated anti-angiogenic activity of this molecule may be associated with inhibition of the interaction with integrins in ECs.

Ocular diseases that are associated with inflammation-associated angiogenesis and lymphangiogenesis can lead to serious problems in the eyes. VEGF and HIF-1α play important roles in the development of pathological corneal and retinal diseases, and they can also alter the expression of drug transporters and the functional activity of carrier transporters (Takagi *et al.*, 1998; Nelson *et al.*, 2003; Wasa *et al.*, 2004; Fradette *et al.*, 2007; Kadam *et al.*, 2013). These events decrease drug delivery and make treatment difficult, thus indicating the importance of regulating inflammation-associated angiogenesis and lymphangiogenesis in eye diseases. Importantly, we observed that *in vivo* treatment with LCB54-0009 effectively suppressed pathological angiogenesis and vascular leakage in retina, but also inflammation-associated neovascularization and lymphangiogenesis in cornea.

In summary, LCB54-0009 is a potent inhibitor of angiogenesis and lymphangiogenesis and the possible mechanisms of its effects are summarized in Figure 8. This compound is an imidazole-based alkaloid that inhibited the levels of HIF-1α and Ang-2 and down-regulated VEGFR-2-signalling cascades. These events resulted in a reduction in the levels of angiogenic factors and inflammatory mediators, leading to inhibition of the capillary-like tube formation in ECs. In addition, LCB54-0009 affected HIF-1α protein stability and HIF-1α/NF-κB redox sensitivity via its antioxidant activities. Furthermore, LCB54-0009 exhibited anti-inflammatory, anti-angiogenic and anti-lymphangiogenic effects in animal models of retinopathy and corneal neovascularization *in vivo*. Altogether, these results suggest a potential therapeutic

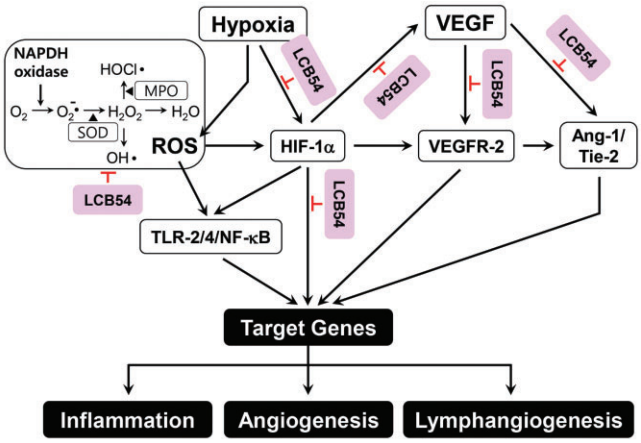

Figure 8

Proposed modes of action of LCB54-0009. LCB54-0009 inhibits ROS-mediated signalling cascades, resulting in the inhibition of HIF-1α, TLR/NF-κB and VEGF/VEGFR-2 signalling pathways. LCB54-0009 also inhibits VEGF-induced Ang-1/Tie-2 signalling cascades. LCB54, LCB54-0009.

effect of LCB54-0009 in the treatment of neovascular eye diseases that are mediated by pathological angiogenesis and lymphangiogenesis.

Acknowledgements

This study was supported by a grant from the Future-Based Technology Development program through the National Research Foundation (NRF) of Korea funded by the Ministry of Education, Science, and Technology (2012–0006131).

Author contributions

B. H. Kim and T. Y. Kim participated the hypothesis and design; B. H. Kim, J. Lee, J. S. Choi and D. Y. Park performed the experiments; H. Y. Song and T. K. Park synthesized compounds; C. H. Cho, S. K. Ye, C. K. Joo, G. Y. Koh and T. Y. Kim provided experimental materials and reagents; B. H. Kim, J. Lee, J. S. Choi and T. Y. Kim analysed the data, discussion of the results and wrote the manuscript.

Conflict of interest

The authors declare no competing financial interest in relation to the work described.

References

Adams RH, Alitalo K (2007). Molecular regulation of angiogenesis and lymphangiogenesis. Nat Rev Mol Cell Biol 8: 464–478.

Alexander SPH, Benson HE, Faccenda E, Pawson AJ, Sharman JL, Spedding, M *et al.* (2013a). The Concise Guide to PHARMACOLOGY 2013/14: catalytic receptors. Br J Pharmacol 170: 1676–1705.

Alexander SPH, Benson HE, Faccenda E, Pawson AJ, Sharman JL, Spedding M *et al.* (2013b). The Concise Guide to PHARMACOLOGY 2013/14: enzymes. Br J Pharmacol 170: 1797–1867.

Arjamaa O, Nikinmaa M (2006). Oxygen-dependent diseases in the retina: role of hypoxia-inducible factors. Exp Eye Res 83: 473–483.

Blouin CC, Pagé EL, Soucy GM, Richard DE (2004). Hypoxic gene activation by lipopolysaccharide in macrophages: implication of hypoxia-inducible factor 1alpha. Blood 103: 1124–1130.

Bock F, Onderka J, Dietrich T, Bachmann B, Kruse FE, Paschke M *et al.* (2007). Bevacizumab as a potent inhibitor of inflammatory corneal angiogenesis and lymphangiogenesis. Invest Ophthalmol Vis Sci 48: 2545–2552.

Bonello S, Zähringer C, BelAiba RS, Djordjevic T, Hess J, Michiels C *et al.* (2007). Reactive oxygen species activate the HIF-1alpha promoter via a functional NFkappaB site. Arterioscler Thromb Vasc Biol 27: 755–761.

Cao Y (2005). Opinion: emerging mechanisms of tumour lymphangiogenesis and lymphatic metastasis. Nat Rev Cancer 5: 735–743.

Cao Z, Shang B, Zhang G, Miele L, Sarkar FH, Wang Z *et al.* (2013). Tumor cell-mediated neovascularization and lymphangiogenesis contrive tumor progression and cancer metastasis. Biochim Biophys Acta 1836: 273–286.

Carmeliet P, Jain RK (2000). Angiogenesis in cancer and other diseases. Nature 407: 249–257.

Castelli MV, Butassi E, Monteiro MC, Svetaz LA, Vicente F, Zacchino SA (2014). Novel antifungal agents: a patent review (2011 – present). Expert Opin Ther Pat 24: 323–338.

Connor KM, Krah NM, Dennison RJ, Aderman CM, Chen J, Guerin KI *et al.* (2009). Quantification of oxygen-induced retinopathy in the mouse: a model of vessel loss, vessel regrowth and pathological angiogenesis. Nat Protoc 4: 1565–1573.

Cueni LN, Detmar M (2006). Insights into the molecular control of the lymphatic vascular system and its role in disease. J Invest Dermatol 126: 2167–2177.

Duan YT, Wang ZC, Sang YL, Tao XX, Zhu HL (2013). Exploration of structure-based on imidazole core as antibacterial agents. Curr Top Med Chem 13: 3118–3130.

Fagiani E, Christofori G (2013). Angiopoietins in angiogenesis. Cancer Lett 328: 18–26.

Felcht M, Luck R, Schering A, Seidel P, Srivastava K, Hu J *et al.* (2012). Angiopoietin-2 differentially regulates angiogenesis through TIE2 and integrin signaling. J Clin Invest 122: 1991–2005.

Ferrara N, Gerber HP, LeCouter J (2003). The biology of VEGF and its receptors. Nat Med 9: 669–676.

Fradette C, Batonga J, Teng S, Piquette-Miller M, du Souich P (2007). Animal models of acute moderate hypoxia are associated with a down-regulation of CYP1A1, 1A2, 2B4, 2C5, and 2C16 and up-regulation of CYP3A6 and P-glycoprotein in liver. Drug Metab Dispos 35: 765–771.

Frank RN (2004). Diabetic retinopathy. N Engl J Med 350: 48–58.

Gao P, Zhang H, Dinavahi R, Li F, Xiang Y, Raman V *et al.* (2007). HIF-dependent antitumorigenic effect of antioxidants *in vivo*. Cancer Cell 12: 230–238.

Gordan JD, Simon MC (2007). Hypoxia-inducible factors: central regulators of the tumor phenotype. Curr Opin Genet Dev 17: 71–77.

Görlach A, Bonello S (2008). The cross-talk between NF-kappaB and HIF-1: further evidence for a significant liaison. Biochem J 412: e17–e19.

Görlach A, Diebold I, Schini-Kerth VB, Berchner-Pfannschmidt U, Roth U, Brandes RP *et al*. (2001). Thrombin activates the hypoxia-inducible factor-1 signaling pathway in vascular smooth muscle cells: role of the p22(phox)-containing NADPH oxidase. Circ Res 89: 47–54.

Grimm C, Willmann G (2012). Hypoxia in the eye: a two-sided coin. High Alt Med Biol 13: 169–175.

Grozdanov V, Müller A, Sengottuvel V, Leibinger M, Fischer D (2010). A method for preparing primary retinal cell cultures for evaluating the neuroprotective and neuritogenic effect of factors on axotomized mature CNS neurons. Curr Protoc Neurosci Chapter 3 (Unit 3.22): 3.22.1–3.22.10.

Haddad JJ, Land SC (2001). A non-hypoxic, ROS-sensitive pathway mediates TNF-alpha-dependent regulation of HIF-1alpha. FEBS Lett 505: 269–274.

Haddad JJ, Olver RE, Land SC (2000). Antioxidant/pro-oxidant equilibrium regulates HIF-1alpha and NF-kappa B redox sensitivity. Evidence for inhibition by glutathione oxidation in alveolar epithelial cells. J Biol Chem 275: 21130–21139.

Hagen T (2012). Oxygen versus reactive oxygen in the regulation of HIF-1α: the balance tips. Biochem Res Int 2012: 436981.

Holmes K, Roberts OL, Thomas AM, Cross MJ (2007). Vascular endothelial growth factor receptor-2: structure, function, intracellular signalling and therapeutic inhibition. Cell Signal 19: 2003–2012.

Kadam RS, Ramamoorthy P, LaFlamme DJ, McKinsey TA, Kompella UB (2013). Hypoxia alters ocular drug transporter expression and activity in rat and calf models: implications for drug delivery. Mol Pharm 10: 2350–2361.

Ke Q, Costa M (2006). Hypoxia-inducible factor-1 (HIF-1). Mol Pharmacol 70: 1469–1480.

Kelly BD, Hackett SF, Hirota K, Oshima Y, Cai Z, Berg-Dixon S *et al*. (2003). Cell type-specific regulation of angiogenic growth factor gene expression and induction of angiogenesis in nonischemic tissue by a constitutively active form of hypoxia-inducible factor 1. Circ Res 93: 1074–1081.

Kietzmann T, Görlach A (2005). Reactive oxygen species in the control of hypoxia-inducible factor-mediated gene expression. Semin Cell Dev Biol 16: 474–486.

Kilkenny C, Browne W, Cuthill IC, Emerson M, Altman DG (2010). Animal research: Reporting *in vivo* experiments: the ARRIVE guidelines. Br J Pharmacol 160: 1577–1579.

Kim Y, Kim BH, Lee H, Jeon B, Lee YS, Kwon MJ *et al*. (2011). Regulation of skin inflammation and angiogenesis by EC-SOD via HIF-1α and NF-κB pathways. Free Radic Biol Med 51: 1985–1995.

Kong TT, Zhang CM, Liu ZP (2013). Recent developments of p38α MAP kinase inhibitors as antiinflammatory agents based on the imidazole scaffolds. Curr Med Chem 20: 1997–2016.

Konisti S, Kiriakidis S, Paleolog EM (2012). Hypoxia – a key regulator of angiogenesis and inflammation in rheumatoid arthritis. Nat Rev Rheumatol 8: 153–162.

Lee J, Kim KE, Choi DK, Jang JY, Jung JJ, Kiyonari H *et al*. (2013). Angiopoietin-1 guides directional angiogenesis through integrin αvβ5 signaling for recovery of ischemic retinopathy. Sci Transl Med 5: 203ra127.

Lee JW, Bae SH, Jeong JW, Kim SH, Kim KW (2004). Hypoxia-inducible factor (HIF-1)alpha: its protein stability and biological functions. Exp Mol Med 36: 1–12.

Majmundar AJ, Wong WJ, Simon MC (2010). Hypoxia-inducible factors and the response to hypoxic stress. Mol Cell 40: 294–309.

Maxwell PH, Wiesener MS, Chang GW, Clifford SC, Vaux EC, Cockman ME *et al*. (1999). The tumour suppressor protein VHL targets hypoxia-inducible factors for oxygen-dependent proteolysis. Nature 399: 271–275.

McGrath J, Drummond G, McLachlan E, Kilkenny C, Wainwright C (2010). Guidelines for reporting experiments involving animals: the ARRIVE guidelines. Br J Pharmacol 160: 1573–1576.

Nelson DM, Smith SD, Furesz TC, Sadovsky Y, Ganapathy V, Parvin CA *et al*. (2003). Hypoxia reduces expression and function of system A amino acid transporters in cultured term human trophoblasts. Am J Physiol Cell Physiol 284: C310–C315.

Norrmén C, Tammela T, Petrova TV, Alitalo K (2011). Biological basis of therapeutic lymphangiogenesis. Circulation 123: 1335–1351.

Olsson AK, Dimberg A, Kreuger J, Claesson-Welsh L (2006). VEGF receptor signalling – in control of vascular function. Nat Rev Mol Cell Biol 7: 359–371.

Park SY, Jang WJ, Yi EY, Jang JY, Jung Y, Jeong JW *et al*. (2010). Melatonin suppresses tumor angiogenesis by inhibiting HIF-1alpha stabilization under hypoxia. J Pineal Res 48: 178–184.

Pawson AJ, Sharman JL, Benson HE, Faccenda E, Alexander SP, Buneman OP *et al*.; NC-IUPHAR. (2014) The IUPHAR/BPS Guide to PHARMACOLOGY: an expert-driven knowledgebase of drug targets and their ligands. Nucl Acids Res 42 (Database Issue): D1098–D1106.

Regenfuss B, Bock F, Cursiefen C (2012). Corneal angiogenesis and lymphangiogenesis. Curr Opin Allergy Clin Immunol 12: 548–554.

Richard DE, Berra E, Pouyssegur J (2000). Nonhypoxic pathway mediates the induction of hypoxia-inducible factor 1alpha in vascular smooth muscle cells. J Biol Chem 275: 26765–26771.

Rivers EC, Mancera RL (2008). New anti-tuberculosis drugs with novel mechanisms of action. Curr Med Chem 15: 1956–1967.

Roskoski R Jr (2007). Vascular endothelial growth factor (VEGF) signaling in tumor progression. Crit Rev Oncol Hematol 62: 179–213.

Sapieha P, Joyal JS, Rivera JC, Kermorvant-Duchemin E, Sennlaub F, Hardy P *et al*. (2010). Retinopathy of prematurity: understanding ischemic retinal vasculopathies at an extreme of life. J Clin Invest 120: 3022–3032.

Sceneay J, Liu MC, Chen A, Wong CS, Bowtell DD, Möller A (2013). The antioxidant N-acetylcysteine prevents HIF-1 stabilization under hypoxia *in vitro* but does not affect tumorigenesis in multiple breast cancer models *in vivo*. PLoS ONE 8: e66388.

Semenza GL (2007). Life with oxygen. Science 318: 62–64.

Semenza GL (2013). Cancer-stromal cell interactions mediated by hypoxia-inducible factors promote angiogenesis, lymphangiogenesis, and metastasis. Oncogene 32: 4057–4063.

Semenza GL (2014). Oxygen sensing, hypoxia-inducible factors, and disease pathophysiology. Annu Rev Pathol 9: 47–71.

Simon MP, Tournaire R, Pouyssegur J (2008). The angiopoietin-2 gene of endothelial cells is up-regulated in hypoxia by a HIF binding site located in its first intron and by the central factors GATA-2 and Ets-1. J Cell Physiol 217: 809–818.

Song HY, Kim SJ, Park SH, Lee HS, Park TK, Woo SH *et al*. (2012). Imidazole-based alkaloid derivatives which have angiogenesis inhibition and antioxidant effects and production method thereof. PCT/KR/003103.

Takagi H, King GL, Aiello LP (1998). Hypoxia upregulates glucose transport activity through an adenosine-mediated increase of GLUT1 expression in retinal capillary endothelial cells. Diabetes 47: 1480–1488.

Tammela T, Alitalo K (2010). Lymphangiogenesis: molecular mechanisms and future promise. Cell 140: 460–476.

Wasa M, Wang HS, Shimizu Y, Okada A (2004). Amino acid transport is down-regulated in ischemic human intestinal epithelial cells. Biochim Biophys Acta 1670: 49–55.

Yuan HT, Yang SP, Woolf AS (2000). Hypoxia up-regulates angiopoietin-2, a Tie-2 ligand, in mouse mesangial cells. Kidney Int 58: 1912–1919.

Zelzer E, Levy Y, Kahana C, Shilo BZ, Rubinstein M, Cohen B (1998). Insulin induces transcription of target genes through the hypoxia-inducible factor HIF-1alpha/ARNT. EMBO J 17: 5085–5094.

Supporting information

Additional Supporting Information may be found in the online version of this article at the publisher's web-site:

http://dx.doi.org/10.1111/bph.13177

Figure S1 Chemical structures of the imidazole-based alkaloid derivatives. Twelve derivatives were synthesized and designated as LCB54 series.

Figure S2 Synthetic scheme of LCB54-0009. LCB54-0009 was synthesized from 3,4-dihydrobenzylaldehyde by sequential synthetic procedures. The core-structure of imidazole-based alkaloid derivatives is shown in the box. The detailed synthetic methods and properties of each compound were referred in the Supporting Information and have been previously reported (Song *et al*., 2012).

Figure S3 ^{1}H-NMR spectra of the intermediate compound alcohol I (A), ketone II (B), bromide III (C) and compound IV (D).

Figure S4 LC-MS spectra of the intermediate compound V (A) and ^{1}H-NMR (B), ^{13}C-NMR (C) and LC-MS (D) spectra of the LCB54-0009.

Figure S5 *In vivo* anti-angiogenic activity of imidazole-based alkaloid derivatives. (A) Eight-week-old SD male rats were injected intravitreally with streptozotocin (60 mg·kg^{-1}) to induce experimental diabetic retinopathy and retinal blood vessel leakage was measured by extravasated FITC-dextran staining using fluorescence microscopy, followed by injection with either vehicle (1% DMSO) or each compound (100 μM) into the vitreous body. (B) Corneal neovascularization was induced by the subconjunctival injection of silver nitrate to cauterize the corneas of SD rats. Vehicle (1% DMSO), each compound (50 μg) or Avastin (200 μg) was injected subconjunctivally 3 days after silver nitrate cauterization and measured using an ophthalmic microscope with a digital camera. Avastin was used as a positive control. *P < 0.05 and **P < 0.005 versus control rats. Among the compounds, LCB54-0009 exhibited the strongest suppression of retinal vascular permeability and corneal neovascularization *in vivo*, suggesting a potential candidate molecule of LCB54-0009 on pathological angiogenesis.

Figure S6 Antioxidant activity of imidazole-based alkaloid derivatives. (A) DPPH radical (black bars) and peroxynitrite (grey bars) scavenging activities of each compound were measured by absorbance using a microplate reader. Data are represented as the inhibition % at 30 μM (DPPH) or 50 μM (peroxynitrite), and the values in the bars indicate IC50 values. (B and C) DPPH radical (B) and peroxynitrite (C) scavenging activities of LCB54-0007, LCB54-0009 and LCB54-0012 were represented. Data are represented as the mean ± SD of three independent experiments (n = 3).

Figure S7 Inhibition of the HIFs expression by imidazole-based alkaloid derivatives. (A) ARPE-19 (top) and primary retinal cells (down) were incubated with various concentrations of LCB54-0009 for 24 to 72 h. Cell viability was measured using the WST-1 reagent and the data are represented as the mean ± SD of three independent experiments (n = 3). B. HUVECs were incubated with each compound (20 μM) for 6 h in hypoxic conditions and Western blot analysis was performed. Among the compounds, LCB54-0009 exhibited the strongest inhibition of HIF-1α expression. (C) ARPE-19 and primary retinal cells were incubated with various concentrations of LCB54-0009 for 6 h in hypoxic conditions. The levels of the HIF-1α and HIF-2α were determined by Western blot analysis. GAPDH served as a loading control.

Figure S8 LCB54-0009 exhibits anti-angiogenic activity *in vitro*. ARPE-19 (A) and primary retinal cells (B) were incubated with either vehicle (0.1% DMSO) or LCB54-0009 (20 μM) for 6 h in hypoxic conditions or 72 h in the presence or absence of VEGF (20 ng·mL^{-1}). The mRNA levels were determined by quantitative real-time PCR and the data are represented as the mean ± SD of three independent experiments (n = 3). #P < 0.05 versus vehicle-treated group; *P < 0.05 and **P < 0.005 versus VEGF- or hypoxia-induced group; $^{\dagger\dagger}P$ < 0.005 versus LCB54-0009-treated group.

Figure S9 LCB54-0009 inhibits iNOS expression. A. HUVECs were incubated with either vehicle (0.1% DMSO) or LCB54-0009 (20 μM) for 6 h in hypoxic conditions. The mRNA levels of PHD1 and PHD2 were determined by quantitative real-time PCR and the data are represented as the mean ± SD of three independent experiments (n = 3). #P < 0.05 versus vehicle-treated group. B. HUVECs were incubated with LCB54-0009 in combination with stimuli (LPS 1 μg·mL^{-1}, TNF-α 10 ng·mL^{-1}, IL-1β 5 U·mL^{-1} and IFN-γ 100 U·mL^{-1}) for 36 h. Western blot analysis was performed to determine iNOS expression. GAPDH served as a loading control. C. *In vitro* peroxynitrite scavenging activity was measured as absorbance at 542 nm, followed by addition with Pyrogallol Red.

Table S1 The primer sequences and product sizes used for end-point RT-PCR.